Extracellular Free Water Elevations are Associated with Maternal Cytokine Response in a Nonhuman Primate Maternal Immune Activation Model

Cameron Carter (cscarter@ucdavis.edu)
University of California at Davis
Tyler Lesh
University of California, Davis https://orcid.org/0000-0002-6160-3927
Ana-Maria Iosif
University of California, Davis https://orcid.org/0000-0001-7283-2015
Costin Tanase
University of California, Davis
Roza Vlasova
Amy Ryan
Jeffrey Bennett
Casey Hogrefe
Richard Maddock
https://orcid.org/0000-0001-6392-5519
Daniel Geschwind
UCLA https://orcid.org/0000-0003-2896-3450
Judy Van de Water
University of California, Davis https://orcid.org/0000-0003-1193-5875
A. Kimberley McAllister
University of California at Davis https://orcid.org/0000-0001-9177-9889
Martin Styner
Melissa Bauman
University of California, Davis

Article

Keywords:

Posted Date: September 6th, 2022

DOI: https://doi.org/10.21203/rs.3.rs-2019576/v1

Version of Record: A version of this preprint was published at Molecular Psychiatry on August 15th, 2023.
See the published version at https://doi.org/10.1038/s41380-023-02213-w.

Abstract

Maternal infection has emerged as an important environmental risk factor for neurodevelopmental disorders, including schizophrenia and autism spectrum disorders. Animal model systems of maternal immune activation (MIA) suggest that the maternal immune response plays a significant role in the neurodevelopment and behavioral outcomes of offspring. Extracellular free water is a measure of freely diffusing water in the brain that may be associated with neuroinflammation and impacted by MIA. The present study evaluates the brain diffusion characteristics of male rhesus monkeys (*Macaca mulatta*) born to MIA-exposed dams ($n = 14$) treated with a modified form of the viral mimic polyinosinic:polycytidylic acid at the end of the first trimester. Control dams received saline injections at the end of the first trimester ($n = 10$) or were untreated ($n = 4$). Offspring underwent diffusion MRI scans at 6, 12, 24, 36, and 45 months of age. Offspring born to MIA-exposed dams showed significantly increased extracellular free water in cingulate cortex gray matter starting as early as 6 months of age and persisting through 45 months. Additionally, offspring gray matter free water in this region was significantly correlated with the magnitude of the maternal IL-6 response in the MIA-exposed dams. These findings provide strong evidence for the construct validity of the NHP MIA model as a system of relevance for investigations of the pathophysiology of human neurodevelopmental psychiatric disorders. Elevated free water in individuals exposed to immune activation in utero could represent an early marker of a perturbed or vulnerable neurodevelopmental trajectory.

Introduction

A significant body of evidence implicates maternal infection as one of the most important environmental risk factors for neurodevelopmental disorders, including schizophrenia and autism spectrum disorders [1–6]. Additional evidence implicating neuroimmune mechanisms in neurodevelopmental disorders include genetic links to the major histocompatibility complex, which contains genes that are critical for adaptive immune function [7], and alterations in measures of immune function, such as serum cytokines and chemokines, that have been repeatedly observed in schizophrenia, bipolar disorder, and autism spectrum disorder [5, 8–12].

Given the critical role that neuroimmune mechanisms play in many aspects of normal brain development and healthy synaptic function, these findings have prompted interest in developing preclinical models that can offer better insight into the mechanism by which exposure to these inflammatory factors may increase risk for neurodevelopmental disorders [13, 14]. A large body of evidence from preclinical research using the maternal immune activation (MIA) model suggests that the maternal immune response is the critical link between exposure to a variety of viral and bacterial infections during pregnancy and alterations in fetal brain development [15–22]. In the MIA model, dams are exposed to an immune activating agent during pregnancy, which prompts an immune response and initiates a trajectory of atypical offspring neurodevelopment which is reflected in altered behavior, brain structure, and function in a proportion of offspring. Rodent MIA models manifest a wide range of behavioral and neuroanatomical

phenotypes suggesting that prenatal immune challenge may serve as a “disease primer” that in combination with other genetic or environmental factors may alter neurodevelopmental trajectories [17, 23, 24]. While comparisons between animal models and clinical disorders must be made with caution, MIA-exposed offspring do exhibit changes relevant to schizophrenia, including altered sensorimotor gating, reduced social behaviors, reduced working memory, increased sensitivity to dopamine receptor agonists, and reductions in cortical gray matter [5, 25]. Alterations in fractional anisotropy (FA) have also been identified in MIA-exposed juvenile [26] and adult [27] mice undergoing diffusion MRI, which is a well replicated finding in individuals with schizophrenia[28, 29]. An important recent development in the investigation of neuroimmune mechanisms of altered neurodevelopment is the emergence of a nonhuman primate (NHP) MIA model. This model offers unique advantages due to the increased similarity to human brain structure and function, cognition and social behavior [30]. Initial studies using the NHP MIA model revealed changes in species-typical behavioral development [31, 32] and long-term alterations in the immune responses of offspring born to MIA-exposed dams [33]. Weir and colleagues [34] noted evidence of neuropathology in these offspring, which showed reductions in the diameter of apical dendrites in the dorsolateral prefrontal cortex at 3.5-4 years of age (late adolescence). We have recently reported decreased frontal grey and white matter paired with subtle cognitive impairments in a cohort of MIA-exposed rhesus monkeys that have undergone longitudinal brain and behavior phenotyping [35]. Rhesus macaque offspring exposed to influenza in utero have also been shown to exhibit subtle behavioral changes in early development and reduced overall gray matter, with most significant reductions in cingulate and parietal cortex [36]. Collectively, these studies suggest that rhesus monkeys prenatally exposed to immune challenge exhibit relatively normal patterns of early behavioral development in spite of atypical brain growth and immune system development, though behavioral changes may become more pronounced as they approach puberty, a time that coincides with a sensitive period of neuronal reorganization and plasticity [37]. Recent work by our group [38] using [^{18}F]fluoro-l-m-tyrosine (FMT) positron emission tomography (PET), also reveal that adolescent MIA-exposed offspring show elevations in striatal dopamine, a finding that is widely replicated in schizophrenia [39, 40].

Abnormalities in brain diffusion characteristics, particularly abnormal fractional anisotropy (FA), have been consistently identified in psychiatric disorders, including psychotic and autism spectrum disorders [28, 41–43]. Reductions in FA have been regularly found in patients with schizophrenia, although newer multi-shell diffusion imaging methods offer a more detailed analysis of these neuroanatomical alterations. Pasternak and colleagues previously demonstrated the utility of measuring extracellular free water as a method of adjusting for free water in the calculation of fractional anisotropy [44], and also as a distinct biomarker that may be associated with inflammation. This and work from our own group [45 38] have shown a pattern of increased free water and comparable free water-corrected FA in first episode psychosis samples, while chronic samples appear to show more prominent reductions in FA [46]. Results of recent back-translational work in a MIA-exposed rat model [47] parallel human studies in chronic SZ patients and show increased extracellular free water in the white matter, particularly within the corpus callosum, external capsule, and striatum. However, the effect of MIA on extracellular free water in the

nonhuman primate model has never been examined and offers a greater neuroanatomical and behavioral similarity to human samples.

The goal of the present study is to use brain diffusion characteristics in NHP offspring over the first four years of life to test the hypothesis that offspring of MIA-exposed dams will show higher extracellular free water in gray matter, and specifically frontal and cingulate cortex, consistent with findings previously seen in patients with schizophrenia. Tissue-specific FA (FA-t) will also be examined, but is hypothesized to be less significantly impacted. Finally, we anticipate that maternal immune reactivity, as measured by the peak IL-6 response after injection, will be positively associated with offspring free water measurements.

Materials And Methods

Experimental procedures were developed in collaboration with the veterinary, animal husbandry, and environmental enrichment staff at the California National Primate Research Center (CNPRC) and approved by the University of California, Davis Institutional Animal Care and Use Committee. All attempts were made to promote the psychological well-being of the animals that participated in this research. These efforts included social housing, enriched diet, use of positive reinforcement strategies, and minimizing the duration of daily training/testing sessions.

Animal Selection and MIA Procedures

Pregnant dams between five and twelve years of age were selected from the indoor time-mated breeding colony at the CNPRC and assigned to MIA (n = 14) and control (n = 10 saline treated and n = 4 untreated) groups. Synthetic double-stranded RNA (polyinosinic:polycytidylic acid [Poly IC] stabilized with poly-L-lysine [Poly ICLC]) (Oncovir, Inc.; 0.25 mg/kg i.v.) or sterile saline (equivalent volume to Poly ICLC) was injected at 07:30 hours in the cephalic vein in awake animals on gestational day (GD) 43, 44 and 46. Blood samples collected 6 hours after the second (GD 44) and third (GD 46) Poly ICLC injections confirmed a strong pro-inflammatory cytokine response as indexed by change in IL-6 from baseline samples as described in Vlasova et al. 2021 [35]. In accordance to recent guideline recommendations for improving the reporting of MIA model methods, we have completed the reporting table from Kentner et al. [48] and will be provided upon request. One offspring from the MIA group was euthanized at 6 months of age due to an unrelated health issue and is not included in any free water analyses. A second animal from the MIA group was euthanized at 42 months of age due to an unrelated health condition and therefore does not contribute data at the final timepoint and is not included in the IL-6 correlation.

Rearing Conditions and Husbandry

Infants were raised in individual cages with their mothers, where they had visual access to other mother-infant pairs at all times. For 3 hours each day, one familiar adult male and four familiar mother-infant pairs were allowed to freely interact in a large cage (3 m long x 1.8 m wide x 2 m high) to provide enrichment and facilitate species-typical social development. The infants were weaned from their

mothers at 6 months of age and were continuously paired with a familiar peer from their rearing group. Weanlings continued the same group socialization routine, with the addition of a non-related adult female, through approximately 18 months of age and remained with treatment-matched permanent pairs thereafter. In addition to the longitudinal neuroimaging studies, the offspring participated in behavioral testing paradigms throughout development as described in Vlasova et al. [35].

Neuroimaging

Magnetic resonance images were collected at 6, 12, 24, 36, and 45 months of age using a Siemens Magnetom Skyra 3-T (Davis, California) with an 8-channel coil optimized for nonhuman primate brain scanning (RapidMR, Columbus, Ohio). While twenty-four of the animals were also scanned at one month of age (and three animals at three months), poor image quality and low gray/white T1 image contrast prevented analysis for the present study. Animals were sedated with ketamine for intubation then anesthetized with isoflurane (1.3-2.0%) at varying rates in order to maintain a steady state of anesthesia. Respiration and heart rate were continually monitored throughout imaging by trained CNPRC staff. Three animals showed sensitivity to isoflurane and were consequently sedated with propofol at subsequent time points. Once the animal was placed in and centered at the mid-line of the MR-compatible stereotaxic frame, the 8-channel receiver coil was attached to the stereotaxic frame using a custom connector. The center point of the 8-channel coil was positioned at AP + 10 on the stereotaxic frame and the Skyra table was then “landmarked” at AP + 10 on the stereotaxic frame so that the center of the animal’s brain was at isocenter. Fluids were maintained with saline at a rate of 10 ml/kg/hr for the duration of the MRI scan.

Acquisition Parameters: T1 weighted images (480 sagittal slices) were acquired with TR = 2500 ms, TE = 3.65 msec, flip angle = 7°, field of view 256x256, voxel size during acquisition was 0.6x0.6x0.6 mm which was interpolated during image reconstruction in the scanner to 512x512 voxels with a resolution of 0.3x0.3x0.3 mm. Diffusion data were acquired with the following settings: TR = 5600-msec, echo time = 90 msec, 0.7 mm in-plane resolution, 42 slices at 1.4 mm slice thickness. The sequence included 64 directions acquired F-H with the following b-shells: 11 x b = 0, 23 x b = 500, 22 x b = 900, 19 x b = 1400. Additional b = 0 images were collected in the opposing phase encoding direction to correct for susceptibility-induced distortion.

Image processing: All images were processed without knowledge of group assignment and only with knowledge of age at scan. T1 weighted images were aligned to a common atlas [49], bias field corrected, and brain masked using AutoSeg_3.3.2 [50]. Brain masks were manually corrected if necessary. Following this preprocessing T1 weighted images were segmented into grey matter (GM), white matter (WM) and cerebrospinal fluid (CSF) using NeosegPipeline_v1.0.8 [51]. University of North Carolina lobar parcellation (https://www.nitrc.org/projects/unc_macaque/) [52] was employed to parcellate the tissue segmentations into 24 lobar brain regions using the multi-atlas fusion in AutoSeg_3.3.2 [50]. All segmentation and parcellation results were visually quality controlled.

Diffusion images were thoroughly inspected for artifacts both visually and using DTIPrep [53] to identify slice-wise, interlace-wise and gradient-wise intensity artifacts. Images with artifacts were discarded and the remaining underwent susceptibility-induced distortion correction [54, 55], eddy current correction and realignment using FSL's eddy [56], including rotation of b-matrices. The Dipy diffusion imaging library [57] and included free water elimination model [58] were used to calculate all diffusion metrics. This model expands the typical DTI model and assumes that each voxel contains two components: an anisotropic tissue-bound component and an isotropic extracellular free water component. In this study, we evaluated both the free water component and tissue-specific fractional anisotropy (FA-t), which reflects traditional FA with the free water component eliminated.

Figure 1 depicts the a priori regions of interest that were selected (ROI; whole-brain, prefrontal, frontal, cingulate, and temporal limbic) based on the body of literature highlighting neuroanatomical alterations associated with MIA [59–62]. Free water was examined separately in white and gray matter ROIs and FA-t was examined only in the white matter of each ROI.

Statistical analysis

Statistical analysis employed linear mixed effects models [63] to model free water measures trajectories and to evaluate group differences between 6 and 45 months of age. An advantage of this approach is the ability to use all available data for an individual, to account for the effect of covariates of interest, and to directly model heterogeneous variances (across groups or time). Outcomes were white and gray matter FW and FA-t in whole-brain, prefrontal, frontal, cingulate, and temporal limbic regions. Separate models were fitted for each ROI and to aid model convergence all outcomes were rescaled (by multiplying with 100). We specified a fourth-order orthogonal polynomial model and accounted for within-subject correlation due to the repeatedly measured outcomes using a random intercept and random slopes for the linear up to quadratic trends. This polynomial model was sufficiently complex to describe all the outcomes in our data. Models included fixed effects for group (MIA vs. control), linear, quadratic, cubic, and quartic effects of age at scan (measured in years), and interactions between age effects and group. For each outcome, we conducted a series of likelihood ratio tests to sequentially evaluate the statistical significance of the four age by group interaction effects. Since none of the interaction terms were significant, they were dropped and a main-effects only model was re-estimated. Higher order polynomial terms were sequentially tested and nonsignificant terms were not retained in final models. All models were validated both graphically and analytically. Tests were two-sided, with $\alpha = 0.05$. All analyses were conducted in SAS version 9.4. (SAS Institute Inc., Cary, NC).

Results

MIA Effect and Developmental Trajectories

As reported by Vlasova and colleagues [35], blood samples revealed a strong increase in IL-6 levels from baseline in MIA treated animals compared to controls (Fig. 2). Additionally, there were no significant differences between groups in any gross measure of offspring development, including growth trajectories (weight, crown rump, head circumference), neuromotor reflexes, and overall health. However, as reported in Vlasova et al [35] the MIA treated animals in this study showed measurable cognitive deficits that were selective to tasks requiring high levels of sustained attention and cognitive flexibility, beginning at 18 months of age.

Neuroimaging Results

Summary information for all diffusion measures and regions of interest are presented in Table 1 and results of statistical analyses are summarized in Table 2. Free water ROI analyses revealed a significant main effect of group and time in the cingulate gray matter (Fig. 3), with higher free water in the MIA offspring compared to controls as well as higher free water over time. The group by time interaction was nonsignificant. Other regions of interest showed only significant effects of time, with no significant interactions and a trend increase in whole-brain gray matter free water ($p = .08$). ROI analyses of FA-t in white matter revealed only significant effects of time, with no main effects of group or group by time interactions.

Table 1
Summary of the free water (FW) measures from 6 to 45 months in MIA-exposed and Control offspring.

	Fractional Anisotropy		White Matter FW		Gray Matter FW	
	MIA (n = 13)	Control (n = 14)	MIA (n = 13)	Control (n = 14)	MIA (n = 13)	Control (n = 14)
Whole-brain Measures, Mean (SD)						
6 months	0.352 (0.015)	0.355 (0.010)	0.129 (0.011)	0.121 (0.011)	0.149 (0.016)	0.138 (0.014)
12 months	0.380 (0.015)	0.378 (0.014)	0.128 (0.018)	0.123 (0.016)	0.157 (0.022)	0.152 (0.020)
24 months	0.421 (0.014)	0.427 (0.012)	0.162 (0.007)	0.159 (0.006)	0.203 (0.019)	0.194 (0.016)
36 months	0.436 (0.014)	0.442 (0.011)	0.166 (0.011)	0.165 (0.005)	0.213 (0.018)	0.211 (0.018)
45 months[a]	0.447 (0.013)	0.451 (0.011)	0.168 (0.009)	0.165 (0.007)	0.217 (0.016)	0.208 (0.021)
Prefrontal Measures, Mean (SD)						
6 months	0.367 (0.024)	0.372 (0.013)	0.087 (0.010)	0.080 (0.015)	0.118 (0.016)	0.114 (0.016)
12 months	0.376 (0.022)	0.374 (0.019)	0.080 (0.017)	0.081 (0.017)	0.124 (0.023)	0.121 (0.018)
24 months	0.417 (0.021)	0.412 (0.012)	0.131 (0.012)	0.121 (0.013)	0.174 (0.018)	0.166 (0.017)
36 months	0.423 (0.017)	0.421 (0.013)	0.130 (0.011)	0.129 (0.015)	0.179 (0.020)	0.184 (0.018)
45 months[a]	0.429 (0.016)	0.429 (0.015)	0.129 (0.008)	0.128 (0.011)	0.188 (0.018)	0.182 (0.020)
Frontal Measures, Mean (SD)						
6 months	0.400 (0.012)	0.399 (0.013)	0.107 (0.015)	0.099 (0.014)	0.138 (0.015)	0.132 (0.015)
12 months	0.420 (0.017)	0.417 (0.018)	0.100 (0.020)	0.099 (0.015)	0.142 (0.019)	0.139 (0.020)

Abbreviations: MIA, maternal immune activation; SD, standard deviation. Data are missing for: [a]n = 1 MIA

	Fractional Anisotropy		White Matter FW		Gray Matter FW	
24 months	0.463 (0.017)	0.464 (0.014)	0.142 (0.007)	0.139 (0.006)	0.180 (0.015)	0.180 (0.013)
36 months	0.475 (0.015)	0.477 (0.014)	0.146 (0.010)	0.149 (0.006)	0.186 (0.020)	0.189 (0.016)
45 months[a]	0.484 (0.012)	0.481 (0.016)	0.149 (0.007)	0.147 (0.007)	0.190 (0.015)	0.182 (0.016)
Cingulate Measures, Mean (SD)						
6 months	0.373 (0.023)	0.381 (0.015)	0.099 (0.021)	0.092 (0.018)	0.153 (0.021)	0.134 (0.018)
12 months	0.389 (0.032)	0.390 (0.020)	0.089 (0.028)	0.089 (0.020)	0.162 (0.029)	0.147 (0.027)
24 months	0.424 (0.019)	0.422 (0.023)	0.125 (0.014)	0.112 (0.013)	0.205 (0.029)	0.184 (0.017)
36 months	0.431 (0.020)	0.440 (0.018)	0.120 (0.013)	0.122 (0.013)	0.211 (0.022)	0.205 (0.020)
45 months[a]	0.432 (0.016)	0.444 (0.023)	0.121 (0.008)	0.122 (0.007)	0.217 (0.022)	0.201 (0.022)
Temporal Limbic Measures, Mean (SD)						
6 months	0.347 (0.024)	0.358 (0.020)	0.141 (0.010)	0.138 (0.013)	0.184 (0.013)	0.176 (0.012)
12 months	0.362 (0.021)	0.368 (0.016)	0.149 (0.016)	0.145 (0.020)	0.187 (0.021)	0.185 (0.020)
24 months	0.377 (0.020)	0.390 (0.020)	0.167 (0.021)	0.167 (0.013)	0.215 (0.018)	0.207 (0.013)
36 months	0.403 (0.018)	0.405 (0.019)	0.179 (0.020)	0.179 (0.016)	0.216 (0.016)	0.223 (0.016)
45 months[a]	0.421 (0.019)	0.430 (0.024)	0.181 (0.013)	0.180 (0.014)	0.226 (0.013)	0.223 (0.016)

Abbreviations: MIA, maternal immune activation; SD, standard deviation. Data are missing for: [a]*n* = 1 MIA

Table 2

Summary of the linear mixed effects models[a] examining trajectories of free water (FW) measures from 6 to 45 months in MIA-exposed and Control offspring

	Fractional Anisotropy		White Matter FW		Gray Matter FW	
Model Term	**Estimate (SE)**	**P-value**	**Estimate (SE)**	**P-value**	**Estimate (SE)**	**P-value**
Whole-Brain Measures						
Intercept	91.80 (0.64)	< 0.001	32.80 (0.35)	< 0.001	40.32 (0.75)	< 0.001
MIA (vs. Control)	-0.30 (0.42)	0.48	0.39 (0.22)	0.08	0.77 (0.48)	0.12
Linear	7.91 (0.16)	< 0.001	3.98 (0.24)	< 0.001	6.26 (0.29)	< 0.001
Quadratic	-2.05 (0.15)	< 0.001	-1.20 (0.13)	< 0.001	-1.87 (0.26)	< 0.001
Cubic	0.24 (0.15)	0.10	-0.61 (0.19)	0.002	-0.59 (0.26)	0.03
Quartic	0.50 (0.15)	0.001	0.98 (0.19)	< 0.001	0.76 (0.26)	0.004
Prefrontal Measures						
Intercept	89.62 (0.82)	< 0.001	24.10 (0.44)	< 0.001	34.23 (0.73)	< 0.001
MIA (vs. Control)	0.24 (0.53)	0.65	0.35 (0.29)	0.24	0.36 (0.47)	0.45
Linear	5.30 (0.22)	< 0.001	4.50 (0.23)	< 0.001	6.29 (0.31)	< 0.001
Quadratic	-1.23 (0.20)	< 0.001	-1.58 (0.23)	< 0.001	-1.68 (0.29)	< 0.001
Cubic	-0.35 (0.20)	0.09	-0.95 (0.23)	< 0.001	-0.70 (0.29)	0.02
Quartic	1.00 (0.20)	< 0.001	1.45 (0.23)	< 0.001	1.09 (0.29)	< 0.001
Frontal Measures						
Intercept	100.15 (0.76)	< 0.001	28.45 (0.36)	< 0.001	36.71 (0.70)	< 0.001
MIA (vs. Control)	0.06 (0.49)	0.90	0.09 (0.22)	0.67	0.34 (0.46)	0.46
Linear	7.08 (0.16)	< 0.001	4.45 (0.25)	< 0.001	4.79 (0.27)	< 0.001
Quadratic	-2.01 (0.15)	< 0.001	-1.19 (0.19)	< 0.001	-1.71 (0.24)	< 0.001

Abbreviations: MIA, maternal immune activation, SE = standard error.

[a]Mixed-effects linear regression fitted to13 MIA (n = 1 missing data at 45 months) and 14 control offspring using fourth-order orthogonal polynomial models. To aid model convergence all outcomes were rescaled (by multiplying with 100). Initial models included fixed effects for group (MIA vs. control), linear, quadratic, cubic, and quartic effects of age at scan (measured in years), and interactions between age effects and group. Random intercepts and slopes were used to account for within-animal dependence. Interaction effects were non-significant and therefore not retained in the final models; higher order polynomial effects that were not significant were also not retained in the final models.

	Fractional Anisotropy		White Matter FW		Gray Matter FW	
Cubic	-0.06 (0.15)	0.68	-0.93 (0.19)	< 0.001	-0.64 (0.24)	0.01
Quartic	0.68 (0.15)	< 0.001	1.23 (0.19)	< 0.001	0.87 (0.24)	< 0.001
Cingulate Measures						
Intercept	92.93 (0.99)	< 0.001	24.26 (0.43)	< 0.001	38.93 (1.00)	< 0.001
MIA (vs. Control)	-0.58 (0.64)	0.37	0.13 (0.25)	0.61	1.55 (0.66)	0.03
Linear	5.34 (0.28)	< 0.001	2.76 (0.28)	< 0.001	5.92 (0.34)	< 0.001
Quadratic	-1.42 (0.28)	< 0.001	-0.75 (0.27)	0.006	-1.67 (0.32)	< 0.001
Cubic	–	–	-0.74 (0.31)	0.02	-0.54 (0.31)	0.09
Quartic	–	–	1.06 (0.33)	0.002	0.63 (0.31)	0.048
Temporal Limbic Measures						
Intercept	87.27 (0.98)	< 0.001	36.21 (0.59)	< 0.001	45.37 (0.67)	< 0.001
MIA (vs. Control)	-0.86 (0.64)	0.19	0.15 (0.38)	0.70	0.29 (0.44)	0.52
Linear	5.87 (0.25)	< 0.001	3.64 (0.26)	< 0.001	3.90 (0.25)	< 0.001
Quadratic	–	–	-0.75 (0.26)	0.004	-0.75 (0.24)	0.002
Cubic	–	–	–	–	-0.22 (0.24)	0.35
Quartic	–	–	–	–	0.46 (0.24)	0.053

Abbreviations: MIA, maternal immune activation, SE = standard error.

[a]Mixed-effects linear regression fitted to13 MIA (n = 1 missing data at 45 months) and 14 control offspring using fourth-order orthogonal polynomial models. To aid model convergence all outcomes were rescaled (by multiplying with 100). Initial models included fixed effects for group (MIA vs. control), linear, quadratic, cubic, and quartic effects of age at scan (measured in years), and interactions between age effects and group. Random intercepts and slopes were used to account for within-animal dependence. Interaction effects were non-significant and therefore not retained in the final models; higher order polynomial effects that were not significant were also not retained in the final models.

In order to evaluate whether the magnitude of the maternal immune response played a role in developmental changes in diffusion characteristics of the offspring, we computed Spearman's rank correlations between summaries reflecting relevant and interpretable aspects of IL-6 and FW data. Maternal IL-6 response was summarized by the peak level (i.e., the maximum) after second and third injections, which may be interpreted as a maximum effect of the injection. Free water in ROIs where a significant free water group effect was identified was summarized by calculating the area under the curve for each individual trajectory, standardized by the length in the study. This approach was preferable to

averaging, because the imaging was performed at unequal time intervals and there was small variation in the ages at scan across offspring. These correlations were conducted separately in the two groups, using only the animals who had compete data (12 MIA, 10 Control). As shown in Fig. 4, free water and maternal IL-6 reactivity were significantly correlated in cingulate gray matter (Spearman's $\rho = 0.71$, $p = 0.01$) in the MIA offspring, but not the control group ($\rho = .02$, $p = 0.96$).

Discussion

The present study revealed, for the first time, a pattern of elevated extracellular free water in the cingulate cortex gray matter, in NHP MIA offspring. Furthermore, these elevations emerged as early as 6 months in development and were stably elevated over the 4-year study time period, equivalent to childhood through early adolescence. Non-significant trends for elevated free water were also present in whole-brain gray matter and these free water alterations occurred in the absence of significant differences in white matter integrity as measured using FA-t. Furthermore and importantly, maternal plasma IL-6 levels were significantly associated with elevated FW in the MIA offspring, providing additional evidence for a robust causal link between maternal immune response and subsequent atypical neurodevelopment.

Free water elevations have recently been reported in an MIA rat model [47]. These data parallel the present study in showing free water elevations in the absence of FA-t group differences, suggesting that MIA-induced changes in offspring may be specific to extracellular diffusion characteristics as opposed to white matter integrity per se. Di Biase and colleagues reported higher extracellular free water in the white matter, particularly within the corpus callosum, external capsule, and striatum and did not report analyses of gray matter FW. Importantly, the finding of MIA-induced FA alterations in offspring in rodent models is not consistent. In MIA mouse models, both increases and decreases in FA have been reported depending upon the region examined and the age of the MIA offspring [26, 27, 64]. These studies did not account for the free water component, however, which should ultimately provide better specificity on how these diffusion characteristics are altered.

The findings of the present study are similar to published studies evaluating extracellular free water in chronic and first episode individuals with schizophrenia [38, 45, 46, 65]. As noted above, in those studies free water appears to be elevated in recent onset samples throughout the white and gray matter. It has been argued from the human studies that the presence of increased FW in schizophrenia may reflect the presence of neuroinflammatory or some other neuroimmune perturbation that is present at illness onset. Such an interpretation is arguably indirect as other mechanisms that might lead to increased extracellular volumes in gray and while matter, such as atrophy, could also lead to this result. In an effort to address this concern, recent work by our group identified a relationship between higher free water in a first episode sample and an important antioxidant and free radical buffer in the brain, glutathione [38]. This correlational analysis revealed that individuals with higher free water also showed lower glutathione levels, providing converging evidence for the presence of a measurable neuroinflammatory or neuroimmune perturbation. Recent work by Di Biase and colleagues [47] identified an association between white matter extracellular

free water and proinflammatory peripheral cytokine levels which provides further evidence for immune involvement. Finally, the results of the present study in the MIA nonhuman primate model provide additional support for this interpretation, since manipulation of the maternal immune response at a critical time during pregnancy (a known risk factor for schizophrenia), resulted in a developmental alteration in cingulate FW in the offspring.

The finding that dams with a higher IL-6 response to poly-ICLC gave birth to offspring with higher free water in cingulate cortex also provides a potential mechanism by which MIA may induce changes in offspring neurodevelopment. Studies in rodents have suggested that IL-6 plays a prominent role in mediating MIA-induced changes in fetal brain development and behavior [66]. Additionally, our own recent work in the rodent MIA model has identified individual variation in the maternal immune response as a predictor of the severity of offspring behavioral phenotypes [67]. These data are also in alignment with work by Garay and colleagues [68] that identified increased levels of largely pro-inflammatory cytokines in the brains of MIA mice offspring, particularly in frontal and cingulate cortices. The link to human brain development has also been highlighted by Rasmussen and colleagues [69], who found that higher maternal IL-6 levels were associated with lower FA values in the uncinate fasciculus in neonates very early in development.

Finally, recently reported brain volumetric data from this sample of nonhuman primates showed an early and stable onset of reduced frontal volume in MIA offspring paired with subtle changes in cognitive performance as the animals matured [35]. The non-significant trends for elevated free water present in frontal and prefrontal gray matter lend further support to our observation that the frontal cortex, which is prominently affected in neurodevelopmental disorders such as schizophrenia [70], might be especially vulnerable to prenatal insults such as MIA [34].

The present study has several limitations that must be acknowledged. As with any study involving an animal model, one must use caution in overinterpreting and ascribing direct links to a particular disorder in humans. While many characteristics of the MIA model have face validity as relevant to psychiatric disorders, such as schizophrenia (e.g., elevated striatal dopamine [71, 72], altered prepulse inhibition [66], reduced social behavior [73], and reduced prefrontal brain volume [36]), commonalities are also seen with autism spectrum disorder (e.g., repetitive behaviors and reduced social behavior [73]). The sample size is also relatively modest and as such we had power to detect only moderate to large effects sizes. There is also emerging evidence that sex may play an important role in MIA studies [74, 75], and the present study was limited to male offspring. Studies in a new cohort that will allow us to gain insights into possible sex differences in the nonhuman primate MIA model are currently underway.

These results, together with the anatomical results reported by Vlasova and colleagues [35], provide strong evidence for the construct validity of the NHP MIA model as a system of relevance for investigations of the pathophysiology of human neurodevelopmental psychiatric disorders. Recent theories propose that activation of the immune system during pregnancy may act as a disease primer that leaves the organism

vulnerable to additional environmental insults during development that may increase risk for psychopathology. Elevated free water in individuals exposed to immune activation in utero could represent an early marker of a perturbed or vulnerable neurodevelopmental trajectory. The current MIA NHP cohort will ultimately undergo cellular and molecular analyses of brain tissue, which will enable us to shed more light on the nature of altered neurodevelopment associated with MIA, and its impact on cellular and molecular mechanisms in the NHP brain.

Declarations

Acknowledgments

These studies were supported by the UC Davis Conte Center to CSC (NIMH; P50MH106438). Development of the nonhuman primate model and behavioral characterization of the offspring were supported by (P50MH106438-04S1) to MDB. Cytokine analysis was supported by the Biological and Molecular Analysis Core of the MIND Institute Intellectual and Developmental Disabilities Research Center (P50HD103526). The authors would like to thank Dr. Thorsten Feiweier from Siemens AG, Healthcare for providing the prototype software package for advanced diffusion imaging which was used to acquire data in the present study. Additional support provided by the base grant (RR00169) of the California National Primate Research Center (CNPRC). We thank the veterinary and animal services staff of the CNPRC for care of the animals. Poly ICLC was kindly provided by Dr. Andres Salazar, MD, Oncovir, Washington D.C.

Conflicts of Interest

The authors report no competing financial interests or potential conflicts of interest.

References

1. Brown AS, Hooton J, Schaefer CA, Zhang H, Petkova E, Babulas V *et al.* Elevated maternal interleukin-8 levels and risk of schizophrenia in adult offspring. Am J Psychiatry 2004; **161**(5): 889–895.
2. Stefansson H, Ophoff RA, Steinberg S, Andreassen OA, Cichon S, Rujescu D *et al.* Common variants conferring risk of schizophrenia. Nature 2009; **460**(7256): 744–747.
3. Careaga M, Rogers S, Hansen RL, Amaral DG, Van de Water J, Ashwood P. Immune Endophenotypes in Children With Autism Spectrum Disorder. Biol Psychiatry 2017; **81**(5): 434–441.
4. Gonzalez-Liencres C, Tas C, Brown EC, Erdin S, Onur E, Cubukcoglu Z *et al.* Oxidative stress in schizophrenia: a case-control study on the effects on social cognition and neurocognition. BMC Psychiatry 2014; **14**: 268.
5. Brown AS, Meyer U. Maternal Immune Activation and Neuropsychiatric Illness: A Translational Research Perspective. Am J Psychiatry 2018; **175**(11): 1073–1083.
6. Younga H. Lee, Ph.D.„ Sara Cherkerzian, Sc.D. „ Larry J. Seidman, Ph.D. „ George D. Papandonatos, Ph.D. „ David A. Savitz, Ph.D. „ Ming T. Tsuang, M.D., Ph.D., *et al.* Maternal Bacterial Infection During

Pregnancy and Offspring Risk of Psychotic Disorders: Variation by Severity of Infection and Offspring Sex. American Journal of Psychiatry 2020; **177**(1): 66–75.

7. Sekar A, Bialas AR, de Rivera H, Davis A, Hammond TR, Kamitaki N *et al.* Schizophrenia risk from complex variation of complement component 4. Nature 2016; **530**(7589): 177–183.
8. Han VX, Patel S, Jones HF, Dale RC. Maternal immune activation and neuroinflammation in human neurodevelopmental disorders. Nat Rev Neurol 2021; **17**(9): 564–579.
9. Han VX, Patel S, Jones HF, Nielsen TC, Mohammad SS, Hofer MJ *et al.* Maternal acute and chronic inflammation in pregnancy is associated with common neurodevelopmental disorders: a systematic review. Transl Psychiatry 2021; **11**(1): 71.
10. Miller BJ, Buckley P, Seabolt W, Mellor A, Kirkpatrick B. Meta-analysis of cytokine alterations in schizophrenia: clinical status and antipsychotic effects. Biol Psychiatry 2011; **70**(7): 663–671.
11. Modabbernia A, Taslimi S, Brietzke E, Ashrafi M. Cytokine alterations in bipolar disorder: a meta-analysis of 30 studies. Biol Psychiatry 2013; **74**(1): 15–25.
12. Masi A, Quintana DS, Glozier N, Lloyd AR, Hickie IB, Guastella AJ. Cytokine aberrations in autism spectrum disorder: a systematic review and meta-analysis. Mol Psychiatry 2015; **20**(4): 440–446.
13. Estes ML, McAllister AK. Maternal immune activation: Implications for neuropsychiatric disorders. Science 2016; **353**(6301): 772–777.
14. Guma E, Plitman E, Chakravarty MM. The role of maternal immune activation in altering the neurodevelopmental trajectories of offspring: A translational review of neuroimaging studies with implications for autism spectrum disorder and schizophrenia. Neurosci Biobehav Rev 2019; **104**: 141–157.
15. Gumusoglu SB, Stevens HE. Maternal Inflammation and Neurodevelopmental Programming: A Review of Preclinical Outcomes and Implications for Translational Psychiatry. Biol Psychiatry 2019; **85**(2): 107–121.
16. Bergdolt L, Dunaevsky A. Brain changes in a maternal immune activation model of neurodevelopmental brain disorders. Prog Neurobiol 2019; **175**: 1–19.
17. Meyer U. Neurodevelopmental Resilience and Susceptibility to Maternal Immune Activation. Trends Neurosci 2019; **42**(11): 793–806.
18. Shi L, Tu N, Patterson PH. Maternal influenza infection is likely to alter fetal brain development indirectly: the virus is not detected in the fetus. International journal of developmental neuroscience: the official journal of the International Society for Developmental Neuroscience 2005; **23**(2–3): 299–305.
19. Shi L, Fatemi SH, Sidwell RW, Patterson PH. Maternal influenza infection causes marked behavioral and pharmacological changes in the offspring. J Neurosci 2003; **23**(1): 297–302.
20. Meyer U, Feldon J, Schedlowski M, Yee BK. Immunological stress at the maternal-foetal interface: a link between neurodevelopment and adult psychopathology. Brain Behav Immun 2006; **20**(4): 378–388.

21. Patterson PH. Immune involvement in schizophrenia and autism: etiology, pathology and animal models. Behav Brain Res 2009; **204**(2): 313–321.
22. Urakubo A, Jarskog LF, Lieberman JA, Gilmore JH. Prenatal exposure to maternal infection alters cytokine expression in the placenta, amniotic fluid, and fetal brain. Schizophr Res 2001; **47**(1): 27–36.
23. Knuesel I, Chicha L, Britschgi M, Schobel SA, Bodmer M, Hellings JA *et al.* Maternal immune activation and abnormal brain development across CNS disorders. Nat Rev Neurol 2014; **10**(11): 643–660.
24. Guma E, Bordignon PDC, Devenyi GA, Gallino D, Anastassiadis C, Cvetkovska V *et al.* Early or Late Gestational Exposure to Maternal Immune Activation Alters Neurodevelopmental Trajectories in Mice: An Integrated Neuroimaging, Behavioral, and Transcriptional Study. Biol Psychiatry 2021; **90**(5): 328–341.
25. Meyer U, Feldon J. Epidemiology-driven neurodevelopmental animal models of schizophrenia. Prog Neurobiol 2010; **90**(3): 285–326.
26. Fatemi SH, Folsom TD, Reutiman TJ, Abu-Odeh D, Mori S, Huang H *et al.* Abnormal expression of myelination genes and alterations in white matter fractional anisotropy following prenatal viral influenza infection at E16 in mice. Schizophr Res 2009; **112**(1–3): 46–53.
27. Li Q, Cheung C, Wei R, Cheung V, Hui ES, You Y *et al.* Voxel-based analysis of postnatal white matter microstructure in mice exposed to immune challenge in early or late pregnancy. Neuroimage 2010; **52**(1): 1–8.
28. Kelly S, Jahanshad N, Zalesky A, Kochunov P, Agartz I, Alloza C *et al.* Widespread white matter microstructural differences in schizophrenia across 4322 individuals: results from the ENIGMA Schizophrenia DTI Working Group. Mol Psychiatry 2017.
29. Koshiyama D, Fukunaga M, Okada N, Morita K, Nemoto K, Usui K *et al.* White matter microstructural alterations across four major psychiatric disorders: mega-analysis study in 2937 individuals. Mol Psychiatry 2020; **25**(4): 883–895.
30. Ryan AM, Bauman MD. Primate Models as a Translational Tool for Understanding Prenatal Origins of Neurodevelopmental Disorders Associated With Maternal Infection. Biol Psychiatry Cogn Neurosci Neuroimaging 2022; **7**(5): 510–523.
31. Bauman MD, Iosif AM, Smith SE, Bregere C, Amaral DG, Patterson PH. Activation of the maternal immune system during pregnancy alters behavioral development of rhesus monkey offspring. Biol Psychiatry 2014; **75**(4): 332–341.
32. Machado CJ, Whitaker AM, Smith SE, Patterson PH, Bauman MD. Maternal immune activation in nonhuman primates alters social attention in juvenile offspring. Biol Psychiatry 2015; **77**(9): 823–832.
33. Rose DR, Careaga M, Van de Water J, McAllister K, Bauman MD, Ashwood P. Long-term altered immune responses following fetal priming in a non-human primate model of maternal immune activation. Brain Behav Immun 2017; **63**: 60–70.

34. Weir RK, Forghany R, Smith SE, Patterson PH, McAllister AK, Schumann CM *et al.* Preliminary evidence of neuropathology in nonhuman primates prenatally exposed to maternal immune activation. Brain Behav Immun 2015; **48**: 139–146.
35. Vlasova RM, Iosif AM, Ryan AM, Funk LH, Murai T, Chen S *et al.* Maternal Immune Activation during Pregnancy Alters Postnatal Brain Growth and Cognitive Development in Nonhuman Primate Offspring. J Neurosci 2021; **41**(48): 9971–9987.
36. Short SJ, Lubach GR, Karasin AI, Olsen CW, Styner M, Knickmeyer RC *et al.* Maternal influenza infection during pregnancy impacts postnatal brain development in the rhesus monkey. Biol Psychiatry 2010; **67**(10): 965–973.
37. Hoftman GD, Lewis DA. Postnatal developmental trajectories of neural circuits in the primate prefrontal cortex: identifying sensitive periods for vulnerability to schizophrenia. Schizophr Bull 2011; **37**(3): 493–503.
38. Bauman MD, Lesh TA, Rowland DJ, Schumann CM, Smucny J, Kukis DL *et al.* Preliminary evidence of increased striatal dopamine in a nonhuman primate model of maternal immune activation. Transl Psychiatry 2019; **9**(1): 135.
39. Howes OD, Kambeitz J, Kim E, Stahl D, Slifstein M, Abi-Dargham A *et al.* The nature of dopamine dysfunction in schizophrenia and what this means for treatment. Arch Gen Psychiatry 2012; **69**(8): 776–786.
40. Fusar-Poli P, Meyer-Lindenberg A. Striatal presynaptic dopamine in schizophrenia, part II: meta-analysis of [(18)F/(11)C]-DOPA PET studies. Schizophr Bull 2013; **39**(1): 33–42.
41. Andrews DS, Lee JK, Solomon M, Rogers SJ, Amaral DG, Nordahl CW. A diffusion-weighted imaging tract-based spatial statistics study of autism spectrum disorder in preschool-aged children. J Neurodev Disord 2019; **11**(1): 32.
42. Karlsgodt KH. Diffusion Imaging of White Matter In Schizophrenia: Progress and Future Directions. Biol Psychiatry Cogn Neurosci Neuroimaging 2016; **1**(3): 209–217.
43. Travers BG, Adluru N, Ennis C, Tromp do PM, Destiche D, Doran S *et al.* Diffusion tensor imaging in autism spectrum disorder: a review. Autism Res 2012; **5**(5): 289–313.
44. Pasternak O, Sochen N, Gur Y, Intrator N, Assaf Y. Free water elimination and mapping from diffusion MRI. Magn Reson Med 2009; **62**(3): 717–730.
45. Pasternak O, Westin CF, Bouix S, Seidman LJ, Goldstein JM, Woo TU *et al.* Excessive extracellular volume reveals a neurodegenerative pattern in schizophrenia onset. J Neurosci 2012; **32**(48): 17365–17372.
46. Pasternak O, Westin CF, Dahlben B, Bouix S, Kubicki M. The extent of diffusion MRI markers of neuroinflammation and white matter deterioration in chronic schizophrenia. Schizophr Res 2015; **161**(1): 113–118.
47. Di Biase MA, Katabi G, Piontkewitz Y, Cetin-Karayumak S, Weiner I, Pasternak O. Increased extracellular free-water in adult male rats following in utero exposure to maternal immune activation. Brain Behav Immun 2020; **83**: 283–287.

48. Kentner AC, Bilbo SD, Brown AS, Hsiao EY, McAllister AK, Meyer U *et al.* Maternal immune activation: reporting guidelines to improve the rigor, reproducibility, and transparency of the model. Neuropsychopharmacology 2019; **44**(2): 245–258.
49. Shi Y, Budin F, Yapuncich E, Rumple A, Young JT, Payne C *et al.* UNC-Emory Infant Atlases for Macaque Brain Image Analysis: Postnatal Brain Development through 12 Months. Front Neurosci 2016; **10**: 617.
50. Wang J, Vachet C, Rumple A, Gouttard S, Ouziel C, Perrot E *et al.* Multi-atlas segmentation of subcortical brain structures via the AutoSeg software pipeline. Front Neuroinform 2014; **8**: 7.
51. Cherel M, Budin F, Prastawa M, Gerig G, Lee K, Buss C *et al.* Automatic Tissue Segmentation of Neonate Brain MR Images with Subject-specific Atlases. Proc SPIE Int Soc Opt Eng 2015; **9413**.
52. Styner M, Knickmeyer R, Joshi S, Coe C, Short S, Gilmore J. Automatic Brain Segmentation in Rhesus Monkeys. *Proceedings of SPIE - The International Society for Optical Engineering* 2007; **6512**.
53. Oguz I, Farzinfar M, Matsui J, Budin F, Liu Z, Gerig G *et al.* DTIPrep: quality control of diffusion-weighted images. Front Neuroinform 2014; **8**: 4.
54. Andersson JL, Skare S, Ashburner J. How to correct susceptibility distortions in spin-echo echo-planar images: application to diffusion tensor imaging. Neuroimage 2003; **20**(2): 870–888.
55. Smith SM, Jenkinson M, Woolrich MW, Beckmann CF, Behrens TE, Johansen-Berg H *et al.* Advances in functional and structural MR image analysis and implementation as FSL. Neuroimage 2004; **23 Suppl 1**: S208-219.
56. Andersson JLR, Sotiropoulos SN. An integrated approach to correction for off-resonance effects and subject movement in diffusion MR imaging. Neuroimage 2016; **125**: 1063–1078.
57. Garyfallidis E, Brett M, Amirbekian B, Rokem A, van der Walt S, Descoteaux M *et al.* Dipy, a library for the analysis of diffusion MRI data. Front Neuroinform 2014; **8**: 8.
58. Hoy AR, Koay CG, Kecskemeti SR, Alexander AL. Optimization of a free water elimination two-compartment model for diffusion tensor imaging. Neuroimage 2014; **103**: 323–333.
59. Piontkewitz Y, Arad M, Weiner I. Abnormal trajectories of neurodevelopment and behavior following in utero insult in the rat. Biol Psychiatry 2011; **70**(9): 842–851.
60. Willette AA, Lubach GR, Knickmeyer RC, Short SJ, Styner M, Gilmore JH *et al.* Brain enlargement and increased behavioral and cytokine reactivity in infant monkeys following acute prenatal endotoxemia. Behav Brain Res 2011; **219**(1): 108–115.
61. Crum WR, Sawiak SJ, Chege W, Cooper JD, Williams SCR, Vernon AC. Evolution of structural abnormalities in the rat brain following in utero exposure to maternal immune activation: A longitudinal in vivo MRI study. Brain Behav Immun 2017; **63**: 50–59.
62. Drazanova E, Ruda-Kucerova J, Kratka L, Horska K, Demlova R, Starcuk Z, Jr. *et al.* Poly(I:C) model of schizophrenia in rats induces sex-dependent functional brain changes detected by MRI that are not reversed by aripiprazole treatment. Brain Res Bull 2018; **137**: 146–155.
63. Laird NM, Ware JH. Random-effects models for longitudinal data. Biometrics 1982; **38**(4): 963–974.

64. Fatemi SH, Reutiman TJ, Folsom TD, Huang H, Oishi K, Mori S *et al.* Maternal infection leads to abnormal gene regulation and brain atrophy in mouse offspring: implications for genesis of neurodevelopmental disorders. Schizophr Res 2008; **99**(1–3): 56–70.
65. Lyall AE, Pasternak O, Robinson DG, Newell D, Trampush JW, Gallego JA *et al.* Greater extracellular free-water in first-episode psychosis predicts better neurocognitive functioning. Mol Psychiatry 2017.
66. Smith SE, Li J, Garbett K, Mirnics K, Patterson PH. Maternal immune activation alters fetal brain development through interleukin-6. J Neurosci 2007; **27**(40): 10695–10702.
67. Estes ML, Prendergast K, MacMahon JA, Cameron S, Aboubechara JP, Farrelly K *et al.* Baseline immunoreactivity before pregnancy and poly(I:C) dose combine to dictate susceptibility and resilience of offspring to maternal immune activation. Brain Behav Immun 2020; **88**: 619–630.
68. Garay PA, Hsiao EY, Patterson PH, McAllister AK. Maternal immune activation causes age- and region-specific changes in brain cytokines in offspring throughout development. Brain Behav Immun 2013; **31**: 54–68.
69. Rasmussen JM, Graham AM, Entringer S, Gilmore JH, Styner M, Fair DA *et al.* Maternal Interleukin-6 concentration during pregnancy is associated with variation in frontolimbic white matter and cognitive development in early life. Neuroimage 2019; **185**: 825–835.
70. Smucny J, Dienel SJ, Lewis DA, Carter CS. Mechanisms underlying dorsolateral prefrontal cortex contributions to cognitive dysfunction in schizophrenia. Neuropsychopharmacology 2022; **47**(1): 292–308.
71. Cassidy CM, Carpenter KM, Konova AB, Cheung V, Grassetti A, Zecca L *et al.* Evidence for Dopamine Abnormalities in the Substantia Nigra in Cocaine Addiction Revealed by Neuromelanin-Sensitive MRI. Am J Psychiatry 2020; **177**(11): 1038–1047.
72. Bauman MD, Van de Water J. Translational opportunities in the prenatal immune environment: Promises and limitations of the maternal immune activation model. Neurobiol Dis 2020; **141**: 104864.
73. Malkova NV, Yu CZ, Hsiao EY, Moore MJ, Patterson PH. Maternal immune activation yields offspring displaying mouse versions of the three core symptoms of autism. Brain Behav Immun 2012; **26**(4): 607–616.
74. Scheffler F, Kilian S, Chiliza B, Asmal L, Phahladira L, du Plessis S *et al.* Effects of cannabis use on body mass, fasting glucose and lipids during the first 12months of treatment in schizophrenia spectrum disorders. Schizophr Res 2018; **199**: 90–95.
75. Coiro P, Pollak DD. Sex and gender bias in the experimental neurosciences: the case of the maternal immune activation model. Transl Psychiatry 2019; **9**(1): 90.

Figures

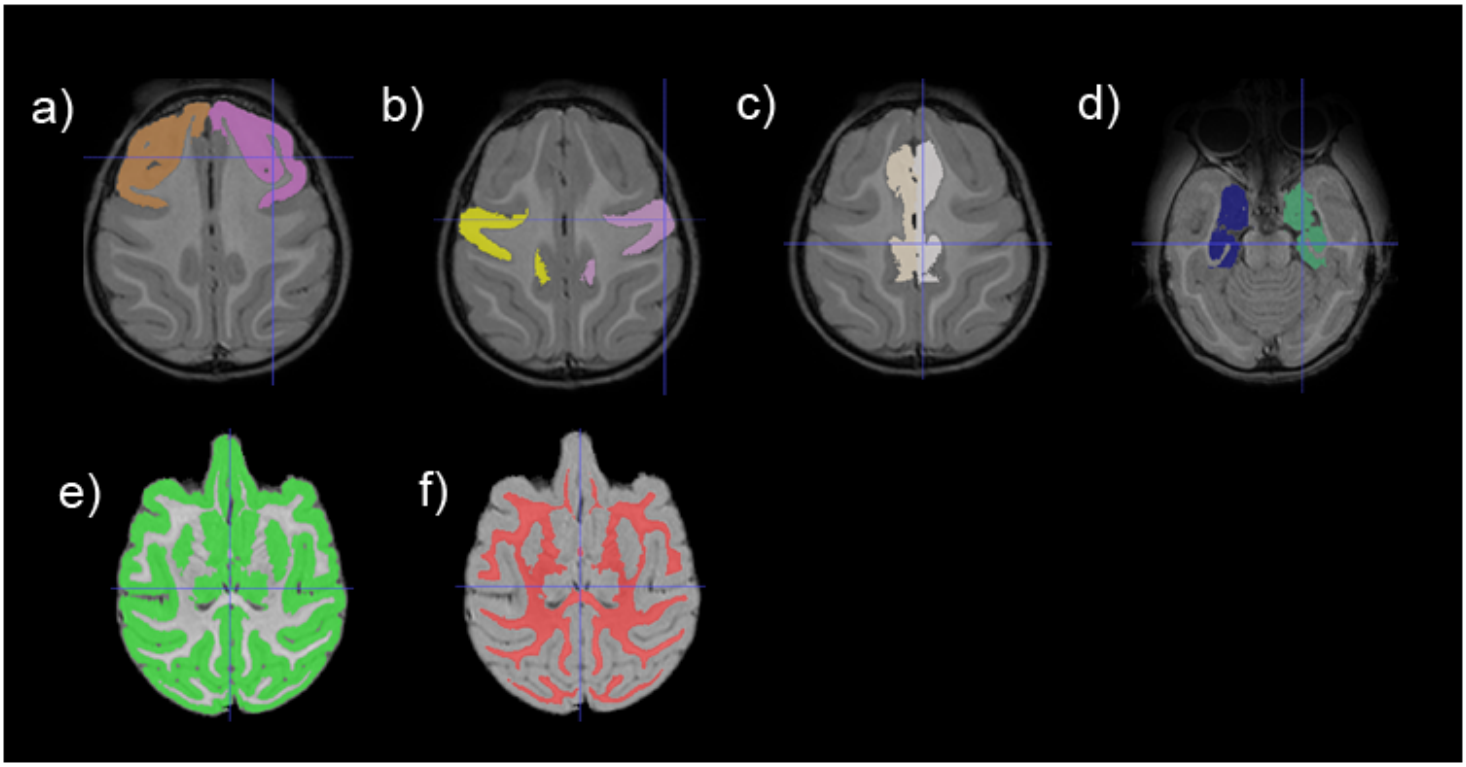

Figure 1

Depiction of regions of interest: a) prefrontal, b) frontal, c) cingulate, d) temporal limbic, e) whole-brain gray matter, and f) whole-brain white matter.

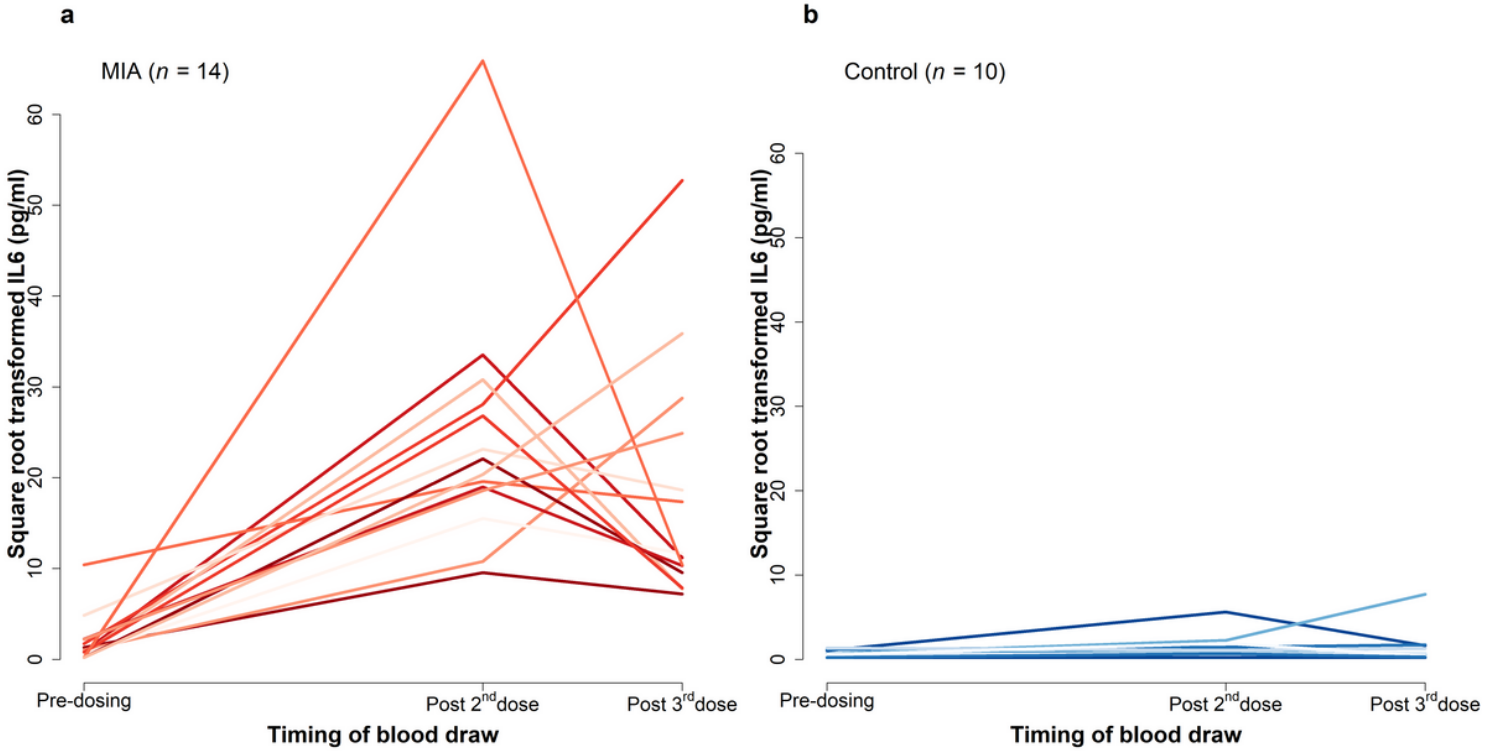

Figure 2

Depiction of peripheral blood IL-6 response in MIA (a) and control (b) dams after PolyIC: LC or saline injection, respectively.

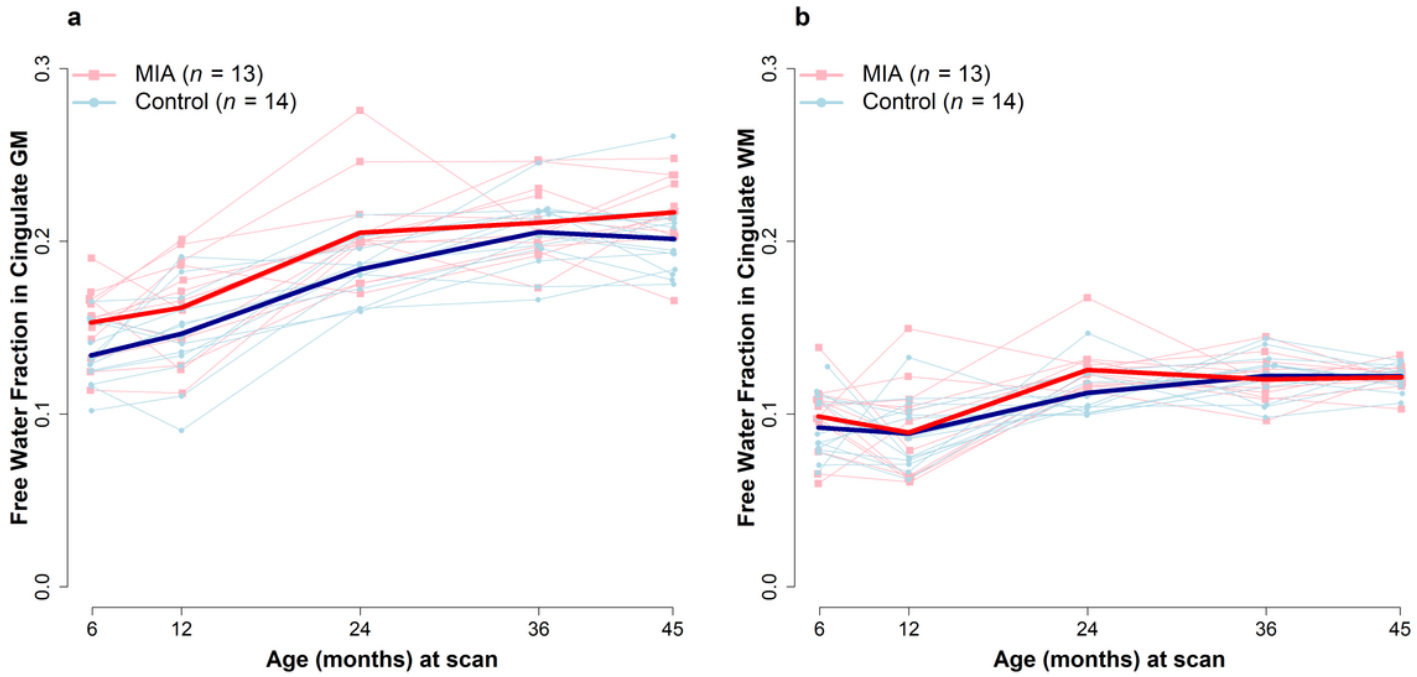

Figure 3

Free water fraction in cingulate gray (a) and white (b) matter across time in MIA-exposed (red) and Control (blue) offspring.

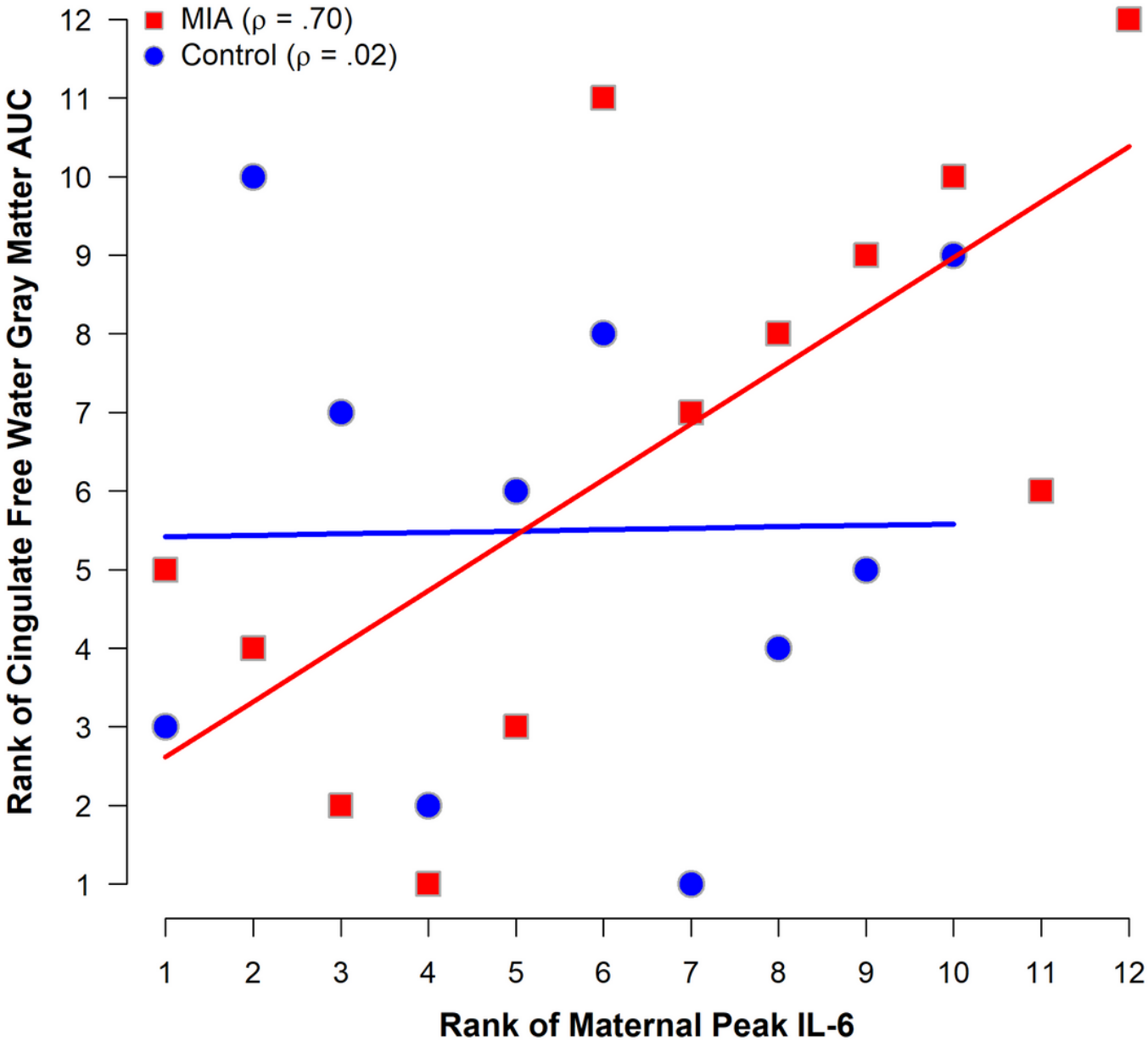

Figure 4

Correlations between summary measure of free mater fraction in cingulate gray matter and maternal immune response in MIA-exposed and Control offspring. Graph shows rank transformed data and Spearman (ρ) correlations.